JET-P(94)70

The Rapid Determination of Plasma Eqyuilibrium Parameters at JET from External Magnetic Measurements

J J Ellis, J P Christiansen, D P J O'Brien, W P Zwingmann, E van der Goot, M Garribba, F Milani, S Puppin, F Sartori.

JET Joint Undertaking, Abingdon, Oxfordshire, OX14 3EA, UK.

Preprint of a paper to be submitted for publication in the Proceedings of IAEA TCM on Magnetic Diagnostics for Fusion Plasmas, (Kharkov, Ukraine, 5-7 October 1994)

December 1994

Abstract.

The control of the plasma shape and position in a tokamak requires a fast, reliable and sufficiently accurate method of determining the plasma boundary. At JET, a method using Taylor series expansions of the magnetic flux surrounding the plasma has been developed which meets these requirements: the calculation takes 1 ms per time slice and comparisons with Langmuir probe and CCD camera data suggest the accuracy is approximately 1 cm, comparable with the full Grad-Shafranov equilibrium codes in use at JET (EFIT, IDENT).

The expansion method has been adapted for use in the pumped divertor phase at JET where it is now used as part of the control software for the plasma shape and position system. The plasma boundary data (position and poloidal field) is also supplied to the FAST code to calculate some global parameters such as poloidal beta, internal inductance and plasma energy. Good agreement with calculations based on diamagnetic measurements is obtained. This information could now be used to control the plasma beta or energy and extend the duration of H- and VH-modes. The representation of the plasma boundary within FAST based on the Lao-Hirshman expressions has been extended to give a better description of the asymmetric single null plasmas which are now predominant at JET.

Introduction.

The analysis of the plasma characteristics in JET, crucial to improving its fusion performance, relies heavily upon a knowledge of the plasma position, shape, energy and other global parameters. These parameters are inferred from various magnetic measurements made by a diagnostic which has recently been upgraded for the pumped divertor phase at JET [1]. This paper describes the first stages of how data from the magnetic diagnostic KC1D at JET is processed during and after a pulse to obtain values for these global parameters.

Location and type of magnetics measurements at JET.

The principal characteristics of the magnetic diagnostic KC1D at JET are described in [1]. In summary, 4 types of measurement are used to determine equilibrium quantities.

1. Full flux loops which measure the total flux relative to the start of the discharge at 4 locations.

2. 3 groups of loops which measure flux differences.

   14 "saddle" coils per octant around the outside of the vessel. Data from 2 opposite octants is available for real time processing.

   11 pairs of coils linking a common marshalling point to positions around the divertor target area (available in real time).

   1 pair of coils linking the marshalling point to a full flux loop (available in real time).

3. 4 groups of signals for measuring the magnetic field.

   18 poloidal measurements per octant, 2 octants available in real time.

   22 pairs of coils in the divertor target area (available in real time).

   7 pairs of coils along the outer poloidal limiter (available in real time).

   10 coils around the inner wall and the top of the vessel (available in real time).

4. 2 diamagnetic loops are being commissioned.

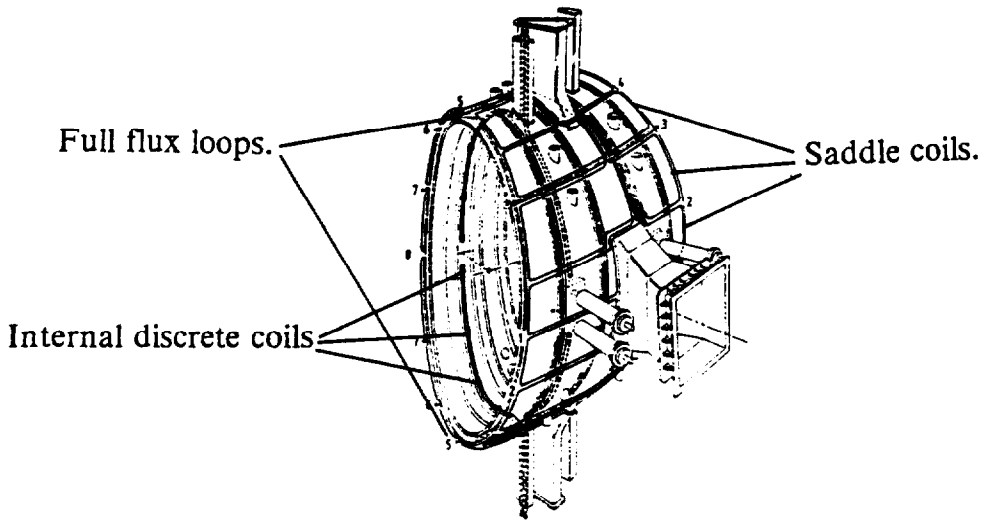

Fig. 1.
Outer magnetic diagnostics at JET.

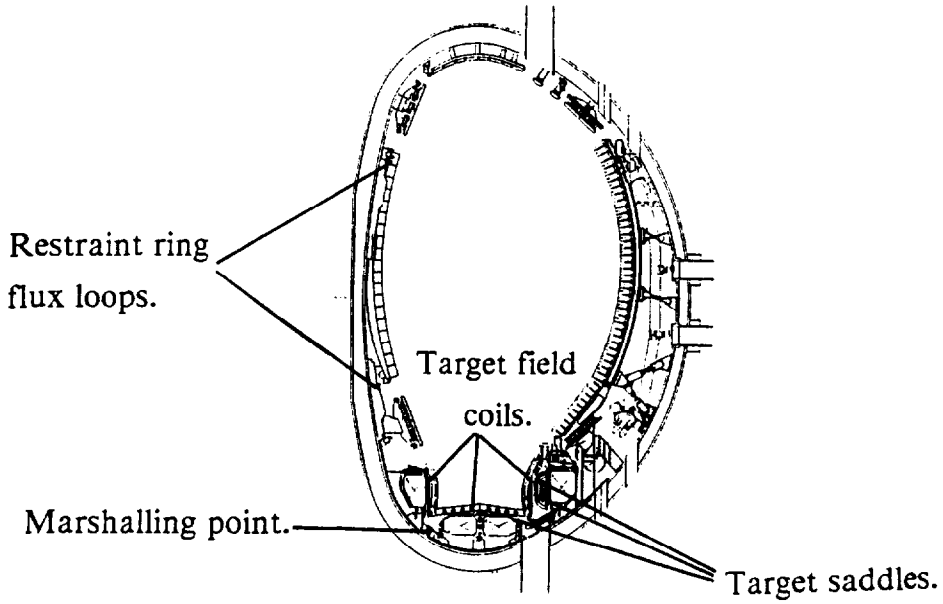

Fig. 2.
Inner magnetic diagnostics at JET.

Data validation and signal preprocessing.

For each signal:

- The initial data offset is found and subtracted. The signal is flagged as bad if the offset > 200 bits.

- The minimum and maximum values of the data are found. The signal is considered bad if:

Maximum - minimum < 20 bits (the signal shows no variation)

Maximum > 30000 or minimum < -30000 bits (16 bit ADCs are used: a value of more than 30000 indicates the signal is saturating due to some fault).

The correction due to toroidal field pickup is found, $c_{sig}I_{TF}$, where I_{TF} is the current in the toroidal field coils and the fixed coefficients c_{sig} are found from special "TF only" pulses. If

$$\max(data) - \min(data) < 0.5c_{sig}(\max I_{TF} - \min I_{TF})$$

the signal is considered bad.

The TF component is removed from the data.

If one signal in a pair is marked bad and the other is not, the good signal is used for processing.

Construction of flux values at "saddle" coil positions.

Most of the equilibrium and plasma boundary reconstrucion programs at JET use flux values rather than flux difference data for their calculations. The flux values are found as follows:

The outer 14 saddle coils are first corrected so that their sum is 0:

$$s_i = s_i - \frac{1}{14}\sum_{k=1}^{14} s_k$$

Fluxes at the outer saddle coil positions are then found by adding or subtracting adjacent saddles e.g.

$$F_1 = F_5 + s_4 + s_3 + s_2 + s_1$$

$$F_7 = F_5 - s_5 - s_6$$

Where F_5 is the measured flux at position 5, F_1 and F_7 are the reconstructed flux values at positions 1 and 7, and s_i are the measured flux differences between positions i and i+1.

Fluxes in the divertor target area are found using the lower restraint ring flux loop and the link coil (see fig. 2):

$$F_t = F_{lrr} - s_{link} - s_t$$

Where F_t is the reconstructed flux in the divertor target area, F_{lrr} is the measured flux at the lower restraint ring, s_{link} is the measured flux difference between the lower restraint ring and the marshalling point, and s_t is the measured flux difference between the marshalling point and one of 11 positions around the divertor target.

Determination of the plasma boundary (XLOC).

This is based on the method described in [2]. The flux function ψ (poloidal flux $/2\pi$) of an axisymmetric plasma can be expanded in a Taylor series about a point (r_0,z_0) up to 6th order

$$\psi = a_1 + a_2\tilde{\rho} + a_3\tilde{z} + \cdots + a_{28}\tilde{z}^6$$

$$\rho = r^2,\ \tilde{\rho} = \rho - r_0^2,\ \tilde{z} = z - z_0$$

Assuming no current flows in the region between the plasma boundary and the measurement positions, then ψ satisfies the Laplace equation

$$4\rho\frac{\partial^2\psi}{\partial\rho^2} + \frac{\partial^2\psi}{\partial z^2} = 0$$

This gives 15 linear constraints on the parameters a_i which can be used to eliminate 15 of the a_i from the expression for ψ. Denoting the 13 remaining coefficients as c_i and grouping the terms involving $\tilde{\rho}^m\tilde{z}^n$ together, then ψ can be written as

$$\psi = c_1 + c_2 f_2(\tilde{\rho}) + \cdots + c_{13} f_{13}(\tilde{\rho}, \tilde{z})$$

$$f_2(\tilde{\rho}) = \tilde{\rho},\ a_2 = c_2,\ a_6 = -4r_0^2 c_4 \ldots$$

The components of the poloidal field, B_r and B_z, can be found from ψ using

$$B_z = 2\frac{\partial\psi}{\partial\rho}, B_r = \frac{-1}{\sqrt{\rho}}\frac{\partial\psi}{\partial z}$$

If the angle between a pickup coil and the horizontal plane is θ, then coefficients b_i can be found which are polynomials in $\tilde{\rho}_m, \tilde{z}_m$, the position of the measurement relative to the centre of the expansion

$$B_{measured} = B_r \cos\theta + B_z \sin\theta = \sum_1^{13} b_i c_i$$

Using at least 13 suitable measurements the coefficients c_i are found by minimising the function

$$\sum_i w_i (D_{(measured)i} - \sum_k d_{ik} c_k)^2$$

where $D_{(measured)i}$ is a measured flux or field value and d_{ik} are the appropriate position dependent polynomials in $\tilde{\rho}, \tilde{z}$ evaluated at the measurement positions.

At JET it has been found that 5 such expansions are needed to describe the plasma boundary, giving a total of 65 coefficients to be determined.

Selection of measurements to be used - the need for extra constraints.

The error caused by truncating the Taylor series at 6th order increases very rapidly $\sim \tilde{\rho}^7$ or $\tilde{z}^7$. The region of validity of an expansion can be seen by studying a contour plot of ψ as there is often an abrupt change in contour direction (fig. 3).

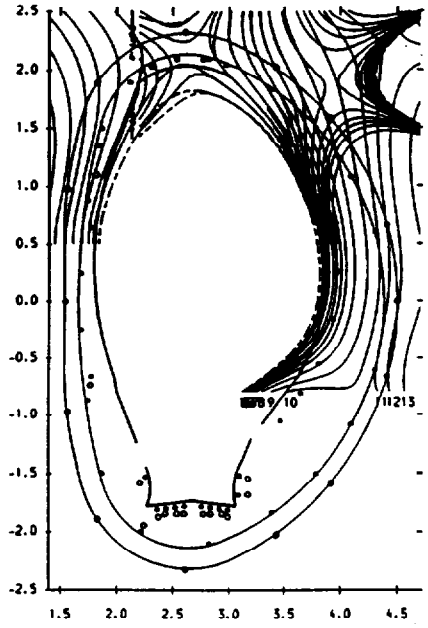

Fig. 3
Overlap of 2 expansions at the top of the vessel
and their region of validity.

The measurements used for the least squares fit should lie within the region of validity of the expansion concerned.

Frequently there are not enough measurements that satisfy this criteria, but by using 5 series for ψ there is usually an area of overlap between adjacent expansions (fig 3).

To overcome the shortage of measurements, additional constraints are introduced such that neighbouring expansions match at some fixed points in the region where the error from both series is sufficiently small ("tie points"). 2 types of constraints are implemented:

1. Adjacent expansions are constrained to agree exactly at a given point, effectively removing 1 coefficient c_i from the least squares fitting procedure.

2. Approximate agreement between adjacent expansions is sought by adding a term

   $w_i(\psi_1(r_i, z_i) - \psi_2(r_i, z_i))^2$

   to the function to be minimised.

Thus after some precalculation, a matrix $\underline{P}$ can be obtained such that

$$\underline{c} = \underline{P}\,\underline{m}$$

where $\underline{c}$ is the vector of coefficients c_i and $\underline{m}$ is the vector of measurements.

Calculation of ψ at the plasma boundary.

The location of any X-points are found using the 28 a_i calculated from the 13 c_i coefficients in the region of interest, by solving

$$\frac{\partial \psi}{\partial \rho} = 0 \text{ and } \frac{\partial \psi}{\partial z} = 0$$

using a Newton-Raphson technique with the initial guess

$$\tilde{\rho} = \frac{2a_2a_6 - a_5a_3}{a_5^2 - 4a_4a_6}, \quad \tilde{z} = \frac{2a_3a_4 - a_2a_5}{a_5^2 - 4a_4a_6}$$

Typically 3 to 5 iterations are needed to converge to an accuracy of 10^{-6} in $\tilde{\rho}$ and $\tilde{z}$.

The value of the flux at the plasma boundary is then found by comparing the flux at the X-points with the flux at 121 limiter points (points inside the private region of the X-points are ignored): the minimum ψ is taken as the value on the boundary of the plasma ($I_{plasma} < 0$)

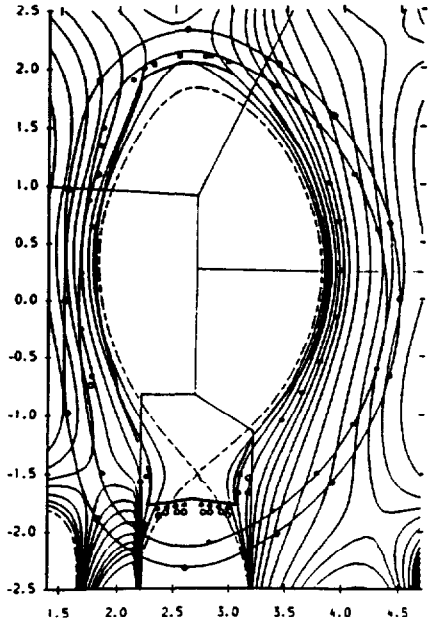

Fig. 4.

Overall flux plot combining the 5 expansions,
showing the boundaries between the 5 expansions.

Summary of algorithm and applications.

After some initialisation, the bulk of the algorithm consists of:

1. a matrix multiply (65x64) to find the 65 coefficients c_i

2. 2 Newton-Raphson calculations to find the X-point positions.

3. 5 matrix multiplies to evaluate the flux at 121 limiter points.

4. $\psi_{bound} = \min(\psi_{XP}, \psi_{lim})$

These calculations can be performed very quickly on modern microprocessors, typically $\sim 1.2ms$ on a T800 transputer network and $<$ 1 ms on a C40 DSP system. This speed, together with the direct nature of the algorithm (which always gives a solution for each time slice) allows the code to be used in real-time applications.

Real time applications of the boundary data.

- A transputer system is used to drive a real-time display of the plasma boundary using a "windows" based interface on a PC [7]

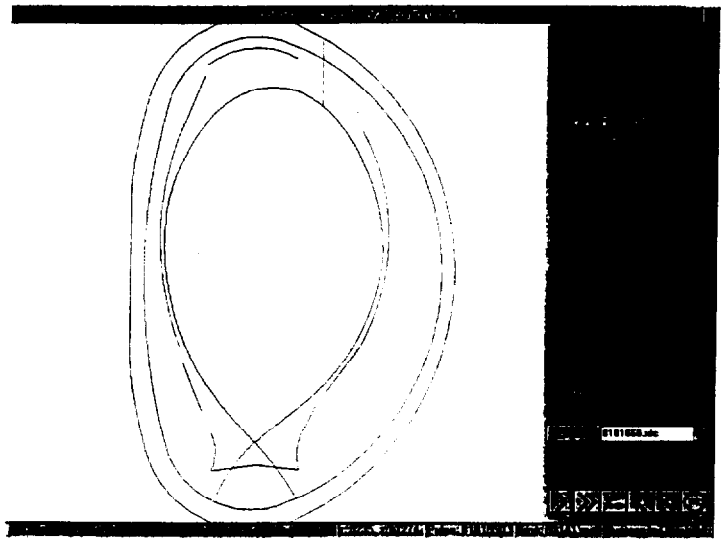

Fig. 5.
Real time display user interface (PC based).

- A C40 based system is used to control the plasma position by monitoring the gaps between the plasma boundary and up to 3 reference points [8].

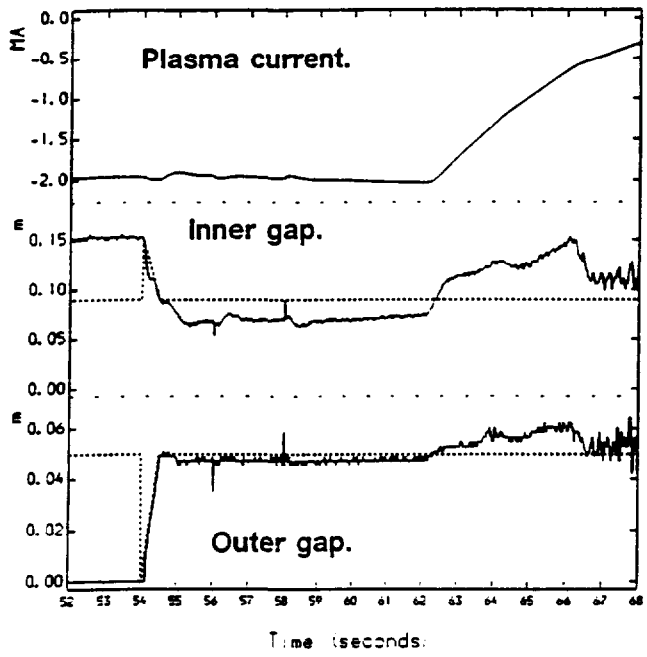

Fig. 6

Example of the use of the algorithm to control the JET plasma during pulse 30667. The dashed lines are the requested gaps, the solid lines the measured gaps.

Effect of errors in the input data.

By replacing each measurement from 1 time slice with a random variable of the same mean value and standard deviation max(0.0025,0.01*mean*), calculating the boundaries and overlaying these results, an estimate of the effect of random errors can be seen.

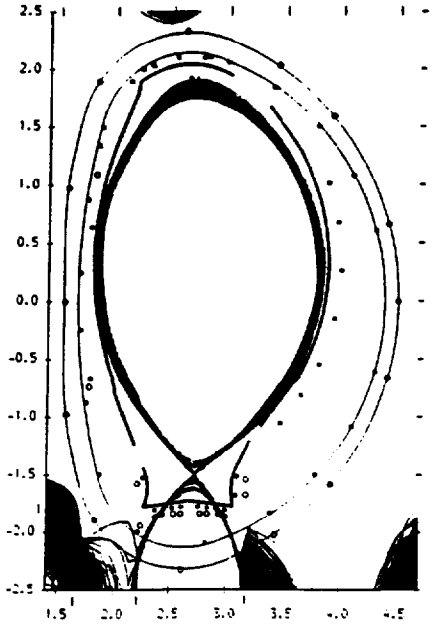

Fig. 7.
Variation in the boundary caused by 1% errors in the data.

As can be seen in fig. 7, the boundary can change by up to $\pm$ 10 cm, although the position of the X-point changes much less. Comparisons with data from Langmuir probes and CCD cameras suggest the error in the position of the strike points is around 1 cm [1].

Effect of errors in the flux loop data data.

As described previously, all the outer flux measurements are referenced to the flux loop at position 5 near the top of the vessel, and all the flux measurements near the target area are referenced to the loop on the lower restraint ring. Unrolling the flux construction, the value of the flux at the lower X-point for pulse 31097 at time 54.209 is

$$\psi_x = 0.00124F_5 + 0.9973F_l + 0.00136F_u + \cdots$$

where F_5 is the measured flux at position 5, F_l the flux at the lower restraint ring and F_u the flux at the upper restraint ring (these are the only absolute flux measurements used). Near the top of the plasma at (3.252,1.55)

$$\psi(3.252,1.55) = 0.9881F_5 + 0.00739F_l + 0.01924F_u + \cdots$$

and $$\frac{\partial \psi}{\partial z} = 0.55$$

Hence an error of 0.056 in F_5 would change the height of the boundary by 10 cm in this case. This flux change is around 2% of the flux swing during the pulse.

Explicit modelling of the JET divertor coils.

To reduce the dependency of the method on the full flux loops the code can be run using the flux difference measurements directly. However, as the marshalling point is beneath the divertor coils the flux and field produced by these must be subtracted from the problem before the constraints derived from the Laplace equation can be used. This can be conveniently achieved by adding 4 parameters (corresponding to the current in each divertor coil) to the list of 65 coefficients to be determined in the least squares fit, and using these to multiply appropriate Greens functions for ψ and $B_{measured}$.

Due to the proximity of the target sensors to the divertor coils (fig. 2), it is important to model the distributed nature of the current in the coils, and this makes calculation of the Greens functions very cpu intensive (this is done using many filamentary loops).

To locate the X-point a null must be found in B_r and B_z where these represent the total field (plasma and coils), and so the Greens functions for this part of the calculation cannot be precalculated. This makes the approach unsuitable for use in real-time for finding the plasma boundary, but increases the region of overlap between adjacent flux expansions near the divertor.

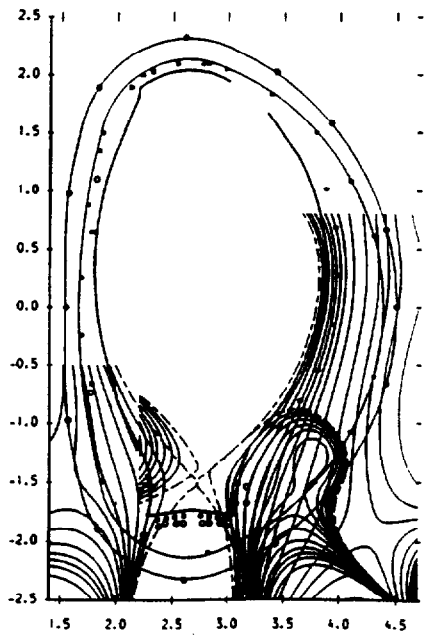

Fig. 8.

Expansion overlap with ψ from divertor coils.

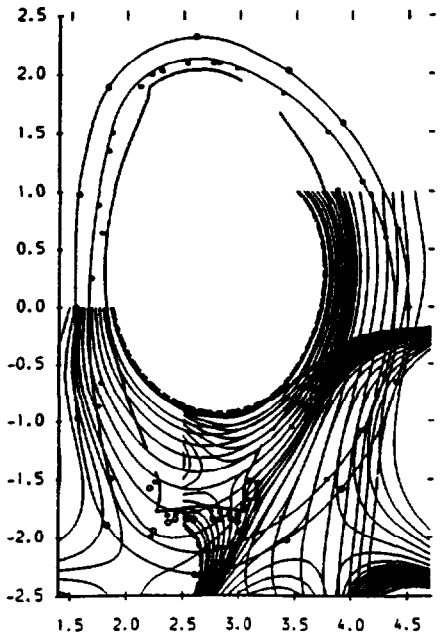

Fig. 9.

Expansion overlap without ψ from divertor coils.

Calculation of current moments.

These are defined by [3] $Y_n = \int (fB_z + grB_n)dl$

Consider such an integral around a fixed path outside the limiters.

$$Y_n = \int \sum_{1}^{65} y_i(r(l),z(l))\, c_i dl \;=\; \sum_{1}^{65} y_i\, c_i$$

By dividing the path of integration into a succession of straight lines the integrals y_i can be calculated analytically, and as details of the plasma boundary are not needed, the solution for the c_i using the divertor model can equally well be used by ignoring the 4 extra terms for the divertor currents.

Overall, the calculation reduces to

$$Y_n = \underline{y}_n \, \underline{P} \, \underline{m}$$

By multiplying out the matrices, this gives a well defined method of calculating the weights needed to find I_p, (r_c, z_c) (the current centroid position) using an arbitrary collection of measurements.

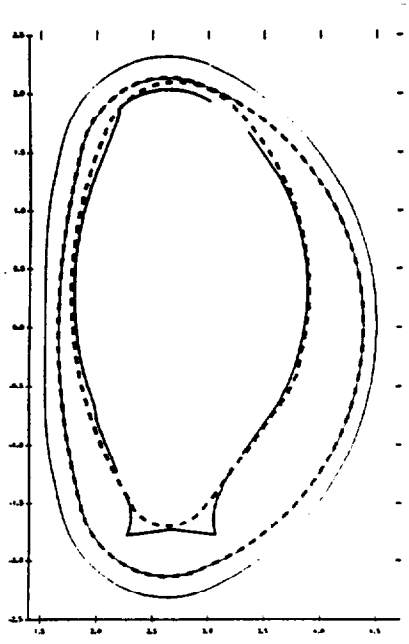

Fig. 10
Integration contours used (shown dotted).

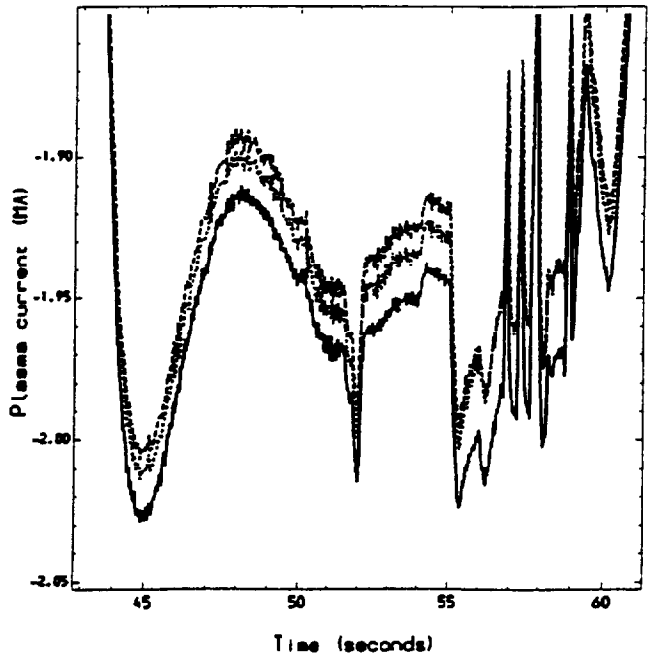

Fig. 11
Plasma current values calculated using this method (dotted),
together with the previous result (full line).

Calculation of plasma inductance, energy.

Once the current centroid (r_c, z_c) has been found one of 9 precalculated polar grids (40x40 points) is used to quickly determine (r,z,B) around the plasma boundary.

The parameter $\Lambda = \beta_i + \ell_i/2$ is found from [4]

$$\Lambda = S_1/2 + (1 - \frac{\delta}{2})S_2, \quad \delta = 1 - r_c/2.96$$

An approximation is then used to find ℓ_i [5]

$$\tilde{l} = 5.8(\frac{1}{2} - \frac{2y_2}{(1-K^2)a^2}) + \frac{2(\Lambda - \frac{\hat{l}}{2})a^2\Lambda}{2.96^2(K^2-1)}(\frac{5+K^2}{4})\alpha_p$$

$$\alpha_p = \min((1 + q_{cyl}/3), 5)$$

$$\hat{l} = \frac{2K}{1+K^2}(0.5 + 0.357\tilde{l})$$

$$\ell_i = 1.4\hat{l} - 0.36$$

where y_2 is the second Shafranov current moment, K is the plasma surface elongation and a the minor radius. From this β_i and hence the plasma energy can then be found. Reasonable agreement is found with values obtained using data from the diamagnetic loop (fig. 12).

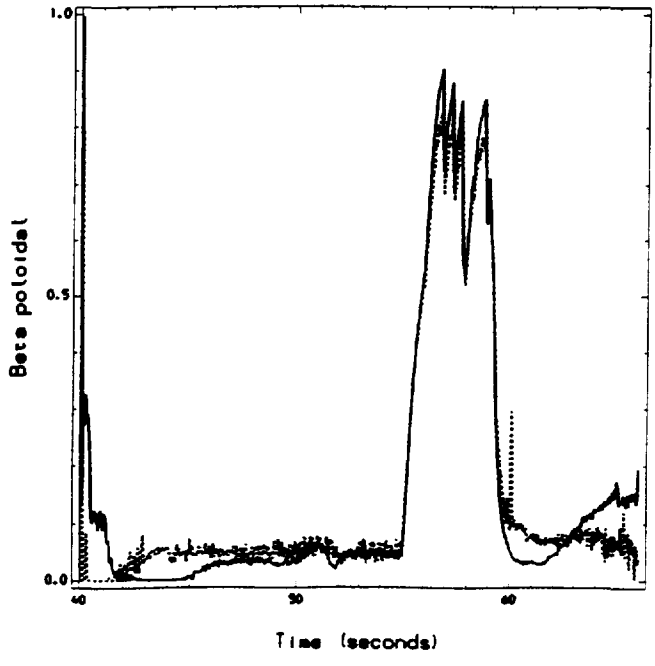

Fig. 12.

Comparison of β_i (solid line) and $\beta_{diamagnetic.}$ (dotted line) for pulse 31097.

Parameterisation of the plasma boundary.

For the analysis of results from other diagnostics, it is convenient to have a compact representation of the plasma boundary.

A generalisation of the analysis used by Weitzner [6] to describe the boundary of a symmetric plasma gives

$$r = R_0 + R_1 \cos\theta + S_1 \sin\theta + \sum_2^{\infty} R_n \cos(n\theta) + S_n \sin(n\theta)$$

$$z = E\,(\, Z_0 + R_1 \sin\theta + S_1 \cos\theta + \sum_2^{\infty} - R_n \sin(n\theta) + S_n \cos(n\theta)\,)$$

Truncating the sums after the terms involving 4θ give a reasonable approximation to the boundary away from the X-point (fig. 13).

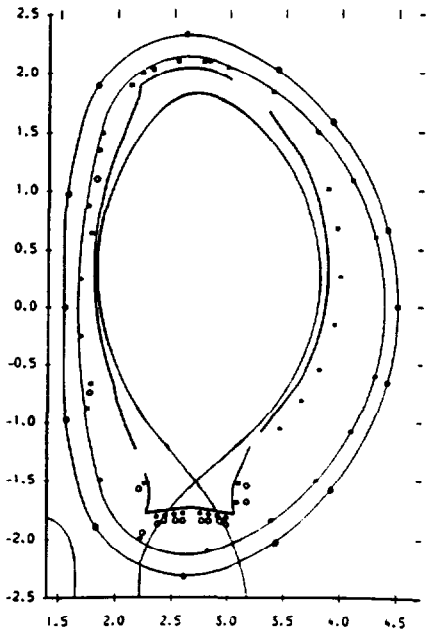

Fig. 13.

Comparison of plasma boundary reconstructed from terms up to 4θ and the original boundary.

Determination of boundary parameters.

The symbol θ in the parameterisation of the plasma boundary represents an arbitrary parameter between 0 and 2π and its functional dependence on the geometric poloidal angle must be found as part of the fitting procedure, which is done as follows:

1. Starting with the set of 40 boundary coordinates $\{(r_b, z_b)\}$, an averaging method is used to find E, r_0 and z_0 and then $\theta = \tan^{-1}(\frac{z_b - z_0}{r_b - r_0})$

2. E, R_n and S_n are then found using a least squares fit technique with fixed values of θ.

3. The values of θ are updated by using 3 iterations of Newton-Raphson to minimise $(r(\theta) - r_b)^2 + (z(\theta) - z_b)^2$ separately at each boundary point.

4. Steps 2 and 3 are repeated 2 times, giving a typical rms error of 1 cm.

Summary and conclusions.

Initial data validation and processing of magnetics data at JET has been outlined. The operation of a fast plasma boundary solver has been described, together with its applications in the plasma control and real-time display systems

The calculation of some global plasma parameters (I_p, r_c, z_c, ℓ_i, β_i) has been described, together with the parameterisation of the plasma boundary.

These techniques are well established, and can be used on a future device (ITER).

Aknowledgements.

The authors would like to thank Drs. J.G. Cordey and R.T. Ross for their support during this work, and members of the Data Management Group for maintaing the data archives: A.J. Capel (JPF), R.A. Layne and P.R.S. Wright (PPF), and P.E. Briden (CPF). We would also like to thank S.A. Arshad and G.F. Neil (and their predecessors) for providing the raw data, and the CODAS division for organising the data acquisition.

References.

[1] S.A. Arshad,"Magnetic Diagnostics for Long Durations", this meeting.

[2] D.P.J. O'Brien, J.J. Ellis, J. Lingertat, "Local Expansion Method for Fast Plasma Boundary Identification at JET', Nuclear Fusion **33** (1993) 467.

[3] L.E. Zakharov, V.D. Shafranov, "Equilibrium of current-carrying plasmas in toroidal configurations." in Reviews of Plasma Physics vol. 11, ed. M.A. Leontovich, Consultants Bureau New York (1986) 153.

[4] V.D. Shafranov,"Determination of the Parameters β_I and ℓ_i in a Tokamak for Arbitrary Shape of Plasma pinch Cross-section", Plasma Physics **13** (1971) 757.

[5] J.P. Christiansen, "Integrated Analysis of Data from JET", J. Comput. Phys., **73** (1987) 85.

[6] L.L. Lao, S.P. Hirshman, R.M. Wieland, "Variational moment solutions to the Grad-Shafranov equation", Phys. Fluids **24** (8) (1981) 1341.

[7] E. v.d. Goot, J.J. Ellis, D.P.J. O'Brien, "A Real Time Plasma Boundary Determination and Display System using Transputers", Proc. 18th Symposium on Fusion Technology (SOFT-18), 1994.

[8] M.Garriba, M.L.Browne, D.J.Campbell, Z.Hudson, R.Litunovsky, V.Marchese, F.Milani, J.Mills, P.Noll, S.Puppin, F.Sartori, L.Scibile, A.Tanga, I.Young, "First Operational Experience with the new Plasma Position and Current Control System at JET.", Proc. 18th Symposium on Fusion Technology (SOFT-18), 1994.